
VersusQ: Pairwise Margin Reasoning for Generalizable Video Quality Assessment

Shibei Meng^{1,3} Binxin Yang² Yuan Liu³ Jiexuan Zhang⁴
Zhengyao Lv⁵ Hubery Yin² Qiang Xu^{1,*}

¹The Chinese University of Hong Kong ²WeChat Vision, Tencent Inc.
³Beijing Normal University ⁴Peking University ⁵The University of Hong Kong

Abstract

Large Multimodal Models (LMMs) have shown promise for video quality assessment, but most methods still predict an absolute score for each video. Such pointwise supervision often mixes perceptual quality with dataset-specific calibration, including annotation protocols, rating habits, and score distributions. As a result, the learned scoring rule may work well within a benchmark but transfer poorly across unseen domains. We argue that relative comparisons alleviate the absolute-scale calibration bias by focusing purely on perceptual differences rather than dataset-specific rating habits. Consequently, we propose **VersusQ**, a pairwise margin reasoning framework driven entirely by direct comparisons. Specifically, VersusQ performs LMM-based comparison between two videos, reasons about their visual and temporal quality differences, and predicts a signed continuous margin that captures both the preferred choice and the degree of difference. Furthermore, to align interpretable comparison rationales with fine-grained numerical differences, we introduce Margin-Coupled GRPO, which jointly optimizes rollout-based relational reasoning and continuous margin regression. Extensive experiments on multiple public VQA benchmarks demonstrate that VersusQ achieves state-of-the-art performance, strong cross-domain generalization, and reliable fine-grained ranking under heterogeneous evaluation scenarios.

1 Introduction

Image Quality Assessment (IQA) and Video Quality Assessment (VQA) aim to predict how humans perceive the visual quality of a given image or video, and have long served as a foundational building block of modern multimedia systems [1, 2]. As video sources grow increasingly diverse in recording environments, compression methods and content types, a practical VQA model is now expected to produce assessments that remain faithful across unseen domains and diverse degradations, such as compression artifacts, color distortion, motion blur, or temporal flickers.

Recent progress in large multimodal models has motivated a series of LMM-based I/VQA methods [3–7]. These methods either map discrete text-defined levels into continuous scores [3, 4], directly generate numerical score tokens, or use reinforcement fine-tuning to incentivize explicit quality reasoning before scoring [5–7]. Despite these advances, a central challenge remains: *generalization*. Most current methods still evaluate each video independently. Such pointwise scoring must learn an absolute scale from datasets whose annotations differ in protocols, rating habits, and score distributions, which makes global comparison across heterogeneous benchmarks difficult.

Pairwise comparison is a natural and important formulation for perceptual quality assessment. It has a long history in ranking and preference modeling [8–10], and has also been explored in IQA/VQA

*Corresponding Author.

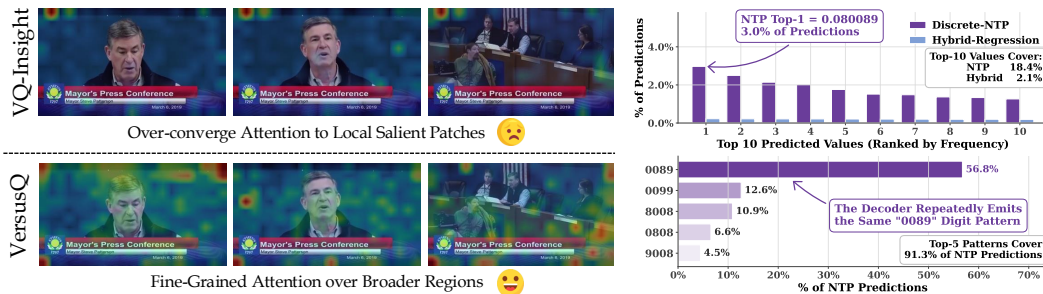


Figure 1: **Two comparisons motivating the proposed design.** Left: under a gradient-based visualization protocol [13], pointwise scoring (*e.g.*, VQ-Inight [14]) concentrates on a few positions, while VersusQ attends more broadly to scene-level evidence. Right: NTP (next-token prediction) directly predicts numeric score tokens and can collapse to repeated outputs, while Hybrid combines reasoning with margin regression to preserve continuous quality differences.

through ranking-based supervision and explicit comparison-to-score designs [11, 12]. The appeal is clear: comparing two videos removes the need to commit to a dataset-specific bias, encourages the model to focus on *relative perceptual evidence*, and better matches how humans judge *subtle quality differences*. As shown by the attention comparison in Figure 1, side-by-side comparison can encourage broader scene-level evidence aggregation than the pointwise scoring.

Despite its clear conceptual appeal, fully transitioning from isolated pairwise experiments to a generalizable VQA leaderboard still gives rise to two central challenges: **(1) From shattered pairs back to a continuous leaderboard.** Pairwise comparisons provide only local, relative information, yet a leaderboard needs globally comparable continuous scores. Binary win/lose labels further discard preference strength (treating marginal and clear wins identically), making fine-grained quality gaps unrecoverable without an impractically large number of comparisons. **(2) Bridging discrete reasoning and continuous quality differences.** While reasoning models can easily generate text to explain their comparisons, they struggle to turn these explanations into precise, continuous magnitudes. When forced to output the difference using next-token prediction (*e.g.*, "...thus A is better by 0.3"), the model often collapses to a few repeated tokens (Figure 1). The core issue is that predicting text token-by-token is simply a poor fit for measuring subtle, continuous quality gaps.

To address the first challenge, we need pairwise supervision to capture not just which response is preferred, but how much better it is, while remaining easy to aggregate into a global leaderboard. Therefore, we introduce the *predictive margin*, a signed real value for each relational comparison that represents the direction and magnitude of the quality gap. At inference time, we consolidate all predicted margins through a closed-form least-squares solution [15], producing a leaderboard that recovers all video scores simultaneously.

Regarding the second challenge, we observe that while language tokens struggle with fine-grained score prediction, the continuous hidden states produced right after the rationale naturally capture the quality gap. Therefore, we attach a lightweight regression head to these post-rationale hidden states for explicit margin prediction. To integrate this objective with policy optimization, we introduce *Margin-Coupled GRPO (MC-GRPO)*, which jointly updates the shared backbone using both rollout-based policy gradients and margin-regression gradients. A brief warm-up stage precedes the unified GRPO loop to initialize the response format and margin regression head.

Our contributions are summarized as follows:

- We propose a generalizable pairwise margin ranking framework built on multimodal relational reasoning, reducing the reliance on domain-specific absolute scores. By formulating training as a pairwise *margin* regression task and reconstructing the full leaderboard via least-squares at inference, our approach focuses on learning relative comparison patterns that can better transfer across evaluation scenarios.
- Moving beyond conventional reasoning-only GRPO paradigms, we introduce **Margin-Coupled GRPO (MC-GRPO)**, which accumulates the policy gradient and the continuous margin-regression gradient within the same optimization update. This strategy jointly trains the shared reasoning backbone and the regression head, ensuring fine-grained numerical eval-

uations are backed by interpretable relational rationales and thereby significantly enhancing the reliability of the resulting ranking.

- Extensive experiments demonstrate that our approach achieves state-of-the-art performance across multiple mainstream benchmarks, with strong cross-domain generalization and reliable fine-grained ranking under heterogeneous evaluation scenarios.

2 Related Work

Image and Video Quality Assessment. Image Quality Assessment (IQA) and Video Quality Assessment (VQA) have progressed from classical metrics such as PSNR, SSIM [16], MOVIE [17], VMAF [18], and ST-RRED [19] to CNN- and transformer-based models [20–25] trained on large-scale perceptual annotations. Large multimodal models (LMMs) [26–28] further enable language-conditioned quality assessment: Q-Align [3] maps discrete textual levels to continuous scores, DeQA-Score [4] softens level labels to reduce discretization loss, and VQA² [29] builds instruction data for joint quality scoring and understanding. Recent methods also elicit explicit quality reasoning with GRPO, including Q-Insight [5], VisualQuality-R1 [6], and VQA-Thinker [7], while RALI [30] uses reasoning traces as intermediate representations for prediction. Nevertheless, most methods still score individual videos independently, limiting fine-grained ranking and adaptation to new domains. Compare2Score [12] mitigates this issue with pairwise comparison, but its five-level quantization limits granularity and interpretability.

Reinforcement Learning for Large Multimodal Models. Reinforcement learning from human feedback (RLHF) aligns language models with human preferences by fitting reward models on pairwise comparisons under the Bradley–Terry formulation [31, 32, 8]. Group Relative Policy Optimization (GRPO) [33, 34] removes the separate reward model and estimates advantages from group-level rewards, making reasoning-oriented fine-tuning more efficient. GRPO and related RL pipelines have been adopted for multimodal reasoning: Video-R1 [35] applies rule-based RL to video understanding, OneThinker [36] unifies image and video reasoning across diverse tasks, and general-purpose models such as InternVL3.5 [37] and Qwen3-VL [38] incorporate multi-stage RL into training. Beyond general understanding, Visual-RFT [39] uses verifiable visual rewards for detection and classification, R1-Onevision [40] bridges visual perception and deep reasoning through SFT and RL, and Seg-Zero [41] trains reasoning-guided segmentation with GRPO alone. However, existing RL pipelines for LMMs mainly optimize discrete textual outputs, leaving regression-oriented quality assessment as token-level score generation.

3 Methodology

3.1 Overview

To establish a comprehensive framework for generalizable pairwise video quality assessment, **VersusQ** in Figure 2 organizes the full pipeline from the supervision target to the model architecture and optimization. **(1) Pairwise ranking with predictive margins** defines the signed quality-difference target m_{ij}^* and reconstructs an anchor-free global leaderboard from predicted relative margins through least-squares aggregation. **(2) Supervision for quality differences** specifies how the VLM observes each video pair and receives direct continuous supervision: a motion-aware video pathway injects temporal features into the language model, and a regression head attached to a particular hidden state predicts the margin under a hybrid reasoning-and-regression objective. **(3) Reinforced reasoning for quality assessment** further improves comparison rationales with GRPO while preserving margin calibration through an auxiliary regression gradient in the same update. This organization separates the ranking formulation, the supervised quality-difference learner, and the reinforcement stage that aligns free-form reasoning with quantitative assessment.

3.2 Pairwise Ranking with Predictive Margins

Existing pairwise IQA methods such as Compare2Score [12] already move beyond binary win/lose labels by quantizing pairwise quality differences into discrete comparative levels and recovering scores with anchor-based probabilistic aggregation. However, this discrete comparison signal still

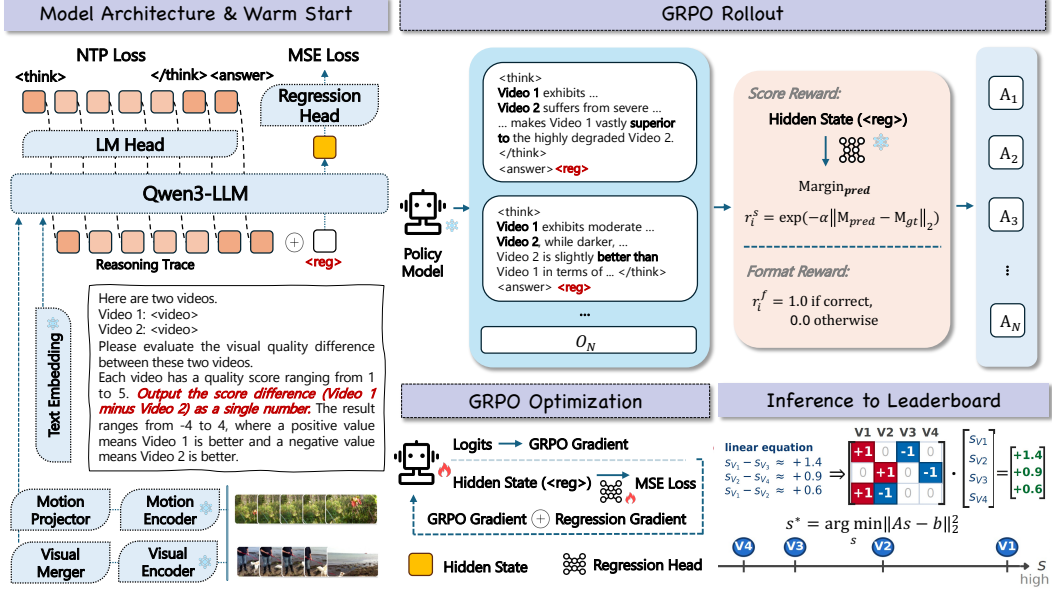


Figure 2: **Overview of the proposed VersusQ pipeline.** VersusQ warm-starts a motion-aware VLM with rationale supervision and MSE margin regression from the designated `<reg>` hidden state. MC-GRPO then uses score and format rewards for reasoning, with an auxiliary regression gradient for calibration. At inference, sparse margins are aggregated into an anchor-free leaderboard by zero-mean least squares.

coarsens fine-grained quality gaps and ties score recovery to predefined anchors. To retain continuous pairwise supervision, we define a ground-truth target margin $m_{ij}^* \in \mathbb{R}$ as the signed difference between the observed Mean Opinion Scores (MOS):

$$m_{ij}^* = s_i^{\text{MOS}} - s_j^{\text{MOS}}, \quad (1)$$

where s_i^{MOS} and s_j^{MOS} are the ground-truth MOS annotations of two videos. The pairwise module predicts \hat{m}_{ij} toward this target, capturing both preference direction and quality-gap magnitude.

At inference time, the model predicts sparse relative margins $\{\hat{m}_{ij}\}$ over N videos and reconstructs leaderboard scores $\mathbf{s} = (s_1, \dots, s_N)^\top$, where s_i denotes the score of video i . Each compared pair (i, j) contributes one linear equation

$$s_i - s_j \approx \hat{m}_{ij}. \quad (2)$$

Stacking these equations over the compared-pair set \mathcal{P} yields an overdetermined system. Let the pairs be indexed by $k = 1, \dots, M$, where $M = |\mathcal{P}|$, and let the k -th pair have indices i_k and j_k . The signed comparison matrix $\mathbf{A} \in \mathbb{R}^{M \times N}$ is

$$A_{k,n} = \begin{cases} +1, & n = i_k, \\ -1, & n = j_k, \\ 0, & \text{otherwise.} \end{cases} \quad (3)$$

Each row of \mathbf{A} therefore encodes one relative comparison, and multiplying it by the score vector extracts the corresponding score difference. The stacked matrix form is

$$\mathbf{A}\mathbf{s} = \begin{bmatrix} s_{i_1} - s_{j_1} \\ s_{i_2} - s_{j_2} \\ \vdots \\ s_{i_M} - s_{j_M} \end{bmatrix} \approx \begin{bmatrix} \hat{m}_{i_1, j_1} \\ \hat{m}_{i_2, j_2} \\ \vdots \\ \hat{m}_{i_M, j_M} \end{bmatrix} = \mathbf{b}. \quad (4)$$

Because predicted margins may be noisy and globally inconsistent, leaderboard scores are obtained by the constrained least-squares problem, following HodgeRank-style least-squares ranking [15]:

$$\mathbf{s}^* = \underset{\mathbf{s} \in \mathbb{R}^N}{\operatorname{argmin}} \|\mathbf{A}\mathbf{s} - \mathbf{b}\|_2^2, \quad \text{s.t.} \quad \sum_i s_i = 0. \quad (5)$$

The zero-mean constraint removes the global shift ambiguity, and the solution satisfies $(\mathbf{A}^\top \mathbf{A}) \mathbf{s}^* = \mathbf{A}^\top \mathbf{b}$ under this gauge constraint. Thus, the leaderboard is **anchor-free**: scores are recovered from predicted-margin consistency without a reference sample. As $|\mathcal{P}|$ increases, the system averages per-pair noise and accumulates finer relative evidence.

3.3 Supervision for Quality Differences

The predictive margin in Sec. 3.2 turns VQA into supervised quality-difference learning: for each video pair, the model must explain the perceptual evidence and predict the signed magnitude of the quality gap. This section first fixes the response format shared by supervised and reinforcement learning, then describes the motion-aware VLM, the regression head, and the supervised objective.

Response Format. For every pairwise prompt x_{ij} , the model follows a fixed response template

$$y_{ij} = \langle \text{think} \rangle \mathbf{c}_{ij} \langle /\text{think} \rangle \langle \text{answer} \rangle \langle \text{reg} \rangle, \quad (6)$$

where \mathbf{c}_{ij} denotes the textual comparison rationale. The $\langle \text{think} \rangle$ block stores the rationale, $\langle \text{answer} \rangle$ ends the response, and $\langle \text{reg} \rangle$ is a non-decoded placeholder exposing the hidden state for continuous margin regression. This template enforces format validity while supporting reasoning supervision and quality-difference prediction.

Motion-Aware VLM Backbone. Temporal artifacts such as motion blur, frame drops, and judder are central to video quality perception, yet standard VLM backbones process only a sparse set of uniformly sampled frames and lack explicit inter-frame dynamics. Inspired by VQA² [29], we integrate a frozen SlowFast R50 [42] encoder through an auxiliary embedding pathway. For each video, a fixed number of T frames is densely sampled and encoded by the frozen motion backbone to capture fine-grained temporal dynamics. The fast-pathway representation is retained and spatially pooled to obtain frame-level motion features $\tilde{\mathbf{u}}_1, \dots, \tilde{\mathbf{u}}_T$. A lightweight motion projector g_θ maps these features into the LLM embedding space:

$$\mathbf{u}_t = g_\theta(\tilde{\mathbf{u}}_t), \quad t = 1, \dots, T, \quad (7)$$

where $\tilde{\mathbf{u}}_t$ is the backbone motion feature and \mathbf{u}_t is the projected motion token. The motion backbone remains frozen, and g_θ is the only trainable component of this pathway.

Regression Head for Quality-Difference Prediction. Directly letting the VLM output a numeric margin causes severe *output quantization* [3]: the model tends to place most probability on a few digit tokens, making the margin too coarse to capture fine-grained quality differences. To avoid this bottleneck, we attach a lightweight MLP regression head to the VLM. Let $\mathbf{h}_{ij} \in \mathbb{R}^d$ denote the hidden state at the $\langle \text{reg} \rangle$ position in Eq. (6). A trainable margin projector r_ϕ maps this hidden state to a continuous margin:

$$\hat{\mathbf{m}}_{ij} = r_\phi(\mathbf{h}_{ij}). \quad (8)$$

Here r_ϕ is the MLP regression head with parameters ϕ , and $\hat{\mathbf{m}}_{ij}$ is the predicted signed quality margin for pair (v_i, v_j) . Because \mathbf{h}_{ij} summarizes the rationale before $\langle \text{answer} \rangle$, margin prediction can use comparison reasoning without discrete digit-token constraints.

Supervised Quality-Difference Learning. Before reinforcement learning, we initialize the response format, motion projector, language model, and regression head with a hybrid next-token prediction and regression objective. Each supervised example is $(v_i, v_j, \mathbf{m}_{ij}^*, \mathbf{c}_{ij})$, where \mathbf{c}_{ij} is a high-level model (*i.e.*, Gemini-3-Pro [43]) annotated rationale. The target response follows Eq. (6). Next-token prediction is applied only to the textual template tokens up to $\langle \text{answer} \rangle$, yielding \mathcal{L}_{NTP} , while the hidden state at $\langle \text{reg} \rangle$ is routed to r_ϕ for margin prediction. For a mini-batch of size B , the regression loss is

$$\mathcal{L}_{\text{reg}} = \frac{1}{B} \sum_{k=1}^B \left\| \hat{\mathbf{m}}^{(k)} - \mathbf{m}^{*(k)} \right\|_2^2, \quad (9)$$

where $\hat{\mathbf{m}}^{(k)}$ and $\mathbf{m}^{*(k)}$ denote the predicted and target margins of the k -th training pair. The final supervised objective is

$$\mathcal{L}_{\text{SFT}} = \mathcal{L}_{\text{NTP}} + \lambda_{\text{reg}} \mathcal{L}_{\text{reg}}, \quad (10)$$

where λ_{reg} controls the strength of the supervised regression term.

3.4 Reinforced Reasoning for Quality Assessment

The supervised objective above provides a strong initialization, but it only teaches the model to imitate fixed reasoning traces. To let the policy explore better comparison rationales while keeping the predicted margin calibrated, we apply **Margin-Coupled GRPO (MC-GRPO)** based on Group Relative Policy Optimization [44]. MC-GRPO uses group-relative rewards to update the rationale-generating policy and uses an auxiliary regression gradient to keep the `<reg>` hidden state predictive of the continuous quality gap.

Rollout and Reward. For a pairwise prompt x_{ij} , the rollout policy $\pi_{\theta_{\text{old}}}$ samples G responses o_1, \dots, o_G in the format of Eq. (6) up to `<answer>`. For each o_g , the `<reg>` placeholder is appended and the regression head predicts $\hat{m}_{ij,g}$. Given the MOS-derived target margin m_{ij}^* , the reward for the g -th response is

$$R_g = \begin{cases} \exp\left(-\alpha \|\hat{m}_{ij,g} - m_{ij}^*\|_2^2\right) + w_f, & \text{if } o_g \text{ has a valid format,} \\ \exp\left(-\alpha \|\hat{m}_{ij,g} - m_{ij}^*\|_2^2\right), & \text{otherwise.} \end{cases} \quad (11)$$

Here α controls sensitivity to squared margin error, and w_f is the format reward for Eq. (6). GRPO estimates the relative advantage by normalizing rewards within the group:

$$\hat{A}_g = \frac{R_g - \text{mean}(\{R_1, \dots, R_G\})}{\text{std}(\{R_1, \dots, R_G\}) + \epsilon_{\text{std}}}, \quad (12)$$

where ϵ_{std} is a small constant for numerical stability.

GRPO Objective. Let π_{θ} , $\pi_{\theta_{\text{old}}}$, and π_{ref} be the current, rollout, and reference policies. For each response, the importance ratio is $\rho_g = \frac{\pi_{\theta}(o_g|x_{ij})}{\pi_{\theta_{\text{old}}}(o_g|x_{ij})}$. The clipped GRPO objective is

$$\mathcal{J}_{\text{GRPO}} = \mathbb{E} \left[\frac{1}{G} \sum_{g=1}^G \left(\min \left(\rho_g \hat{A}_g, \text{clip}(\rho_g, 1 - \epsilon, 1 + \epsilon) \hat{A}_g \right) - \beta D_{\text{KL}}(\pi_{\theta} \parallel \pi_{\text{ref}}) \right) \right]. \quad (13)$$

Here $\mathbb{E}[\cdot]$ denotes expectation over training prompts and sampled responses, ϵ is the clipping threshold, D_{KL} denotes KL divergence, and β controls the KL penalty. The corresponding optimization loss is $\mathcal{L}_{\text{GRPO}} = -\mathcal{J}_{\text{GRPO}}$.

Margin-coupled Update. The policy loss changes the generated rationale, so the final hidden state at `<reg>` may drift away from the representation needed for continuous scoring. MC-GRPO therefore reuses the rollout predictions in the margin MSE of Eq. (9) and optimizes it together with the policy loss. Let θ and ϕ denote the shared VLM/projector parameters and the regression-head parameters, respectively. A single MC-GRPO update is defined as:

$$\begin{aligned} \theta &\leftarrow \theta - \eta (\nabla_{\theta} \mathcal{L}_{\text{GRPO}} + \lambda_{\text{aux}} \nabla_{\theta} \mathcal{L}_{\text{reg}}), \\ \phi &\leftarrow \phi - \eta_{\phi} \lambda_{\text{aux}} \nabla_{\phi} \mathcal{L}_{\text{reg}}. \end{aligned} \quad (14)$$

Here, ∇ denotes the gradient operator, λ_{aux} scales the auxiliary calibration, and η, η_{ϕ} are the respective learning rates. The policy gradient $\nabla_{\theta} \mathcal{L}_{\text{GRPO}}$ optimizes rationale generation, while the auxiliary gradients $\nabla_{\phi} \mathcal{L}_{\text{reg}}$ refine the `<reg>` representation.

4 Experiments

4.1 Experimental Setup

Datasets and metrics. We evaluate VersusQ on seven public VQA benchmarks: LSVQ-test and LSVQ-1080p [45], KoNViD-1k [46], LIVE-VQC [47], LIVE-YT-Gaming [48], Waterloo-IVC-4K [49], and VDPVE [50]. These datasets cover in-the-wild user-generated videos, 1080p and 4K content, gaming videos, codec-induced distortions, and perceptual video enhancement artifacts. Unless otherwise specified, the model is trained on the LSVQ training split and directly evaluated on all target benchmarks, so the non-LSVQ datasets measure cross-dataset generalization. Following VQAThinker [7], we use the entire out-of-domain datasets as test sets (*i.e.*, no train-test split) to comprehensively measure cross-domain generalization. For all datasets, performance is measured by Spearman rank-order correlation coefficient (SRCC) and Pearson linear correlation coefficient (PLCC) between predicted scores and human MOS/DMOS annotations.

Table 1: Quantitative results on in-domain and out-of-domain VQA benchmarks [45–50]. The upper and lower panels report the SRCC and PLCC, respectively. Higher values indicate better performance. **Bold** and underlined values denote the best and second-best results, respectively.

Method	In-domain			Out-of-domain					
	LSVQ-Test	LSVQ-1080p	Avg.	KoNViD	LIVE-VQC	YT-Gaming	W-IVC-4K	VDPVE	Avg.
SRCC									
<i>Training-free / unsupervised quality models</i>									
NIQE [51]	0.442	0.489	0.466	0.541	0.596	0.240	0.048	0.415	0.368
VIIDEO [52]	0.080	0.009	0.044	0.299	0.033	0.077	0.114	0.298	0.164
STEM [53]	0.206	0.434	0.320	0.619	0.594	0.103	0.184	0.389	0.378
CLIP-IQA [54]	0.438	0.553	0.496	0.696	0.704	0.358	0.133	0.415	0.461
<i>Supervised VQA/IQA models</i>									
SimpleVQA [55]	0.864	0.756	0.810	0.861	0.762	0.657	0.379	0.643	0.660
FAST-VQA [23]	0.880	0.781	0.831	0.859	0.826	0.631	0.327	0.611	0.651
DOVER [24]	0.878	0.782	0.830	0.874	<u>0.817</u>	0.647	0.368	0.627	0.667
MinimalisticVQA [56]	<u>0.885</u>	0.792	0.839	0.862	0.775	0.686	0.459	0.639	0.684
Q-Align [3]	0.886	0.761	0.824	0.876	0.783	0.611	0.414	0.639	0.665
VQA ² -Scorer [29]	0.878	0.794	0.836	0.881	0.785	0.613	0.415	0.684	0.676
<i>Reasoning or reinforcement-learning based LMM evaluators</i>									
Q-Insight [5]	0.644	0.601	0.623	0.751	0.624	0.310	0.218	0.547	0.490
VisualQuality-R1 [6]	0.795	0.716	0.756	0.784	0.732	0.472	0.227	0.622	0.567
VQ-Insight [14]	0.875	0.786	0.831	0.875	0.790	N/A	N/A	N/A	N/A
VQAThinker [7]	0.883	<u>0.798</u>	<u>0.841</u>	0.881	0.808	<u>0.767</u>	<u>0.573</u>	<u>0.706</u>	<u>0.747</u>
VersusQ (ours)	0.884	0.824	0.854	<u>0.879</u>	0.801	0.774	0.587	0.723	0.753
PLCC									
<i>Training-free / unsupervised quality models</i>									
NIQE [51]	0.332	0.459	0.396	0.553	0.628	0.247	0.002	0.335	0.353
VIIDEO [52]	0.080	0.019	0.050	0.300	0.215	-0.199	0.078	0.254	0.130
STEM [53]	0.243	0.381	0.312	0.627	0.629	0.111	0.097	0.313	0.355
CLIP-IQA [54]	0.413	0.505	0.459	0.651	0.683	0.384	0.213	0.446	0.475
<i>Supervised VQA/IQA models</i>									
SimpleVQA [55]	0.861	0.801	0.831	0.860	0.799	0.728	0.425	0.647	0.692
FAST-VQA [23]	0.880	0.813	0.847	0.854	0.845	0.677	0.363	0.620	0.672
DOVER [24]	0.866	0.813	0.839	0.869	0.840	0.728	0.418	0.631	0.697
MinimalisticVQA [56]	0.882	0.828	0.855	0.859	0.821	0.746	0.502	0.641	0.714
Q-Align [3]	<u>0.884</u>	0.822	0.853	0.878	0.819	0.681	0.497	0.649	0.705
VQA ² -Scorer [29]	0.872	0.821	0.847	<u>0.880</u>	0.830	0.698	0.474	0.692	0.715
<i>Reasoning or reinforcement-learning based LMM evaluators</i>									
Q-Insight [5]	0.639	0.648	0.643	0.753	0.708	0.326	0.206	0.564	0.511
VisualQuality-R1 [6]	0.796	0.744	0.770	0.792	0.781	0.548	0.298	0.637	0.611
VQ-Insight [14]	0.876	0.823	0.849	0.884	0.835	N/A	N/A	N/A	N/A
VQAThinker [7]	0.880	0.834	<u>0.857</u>	0.884	<u>0.847</u>	0.806	0.624	0.716	0.775
VersusQ (ours)	0.886	0.852	0.869	0.884	0.848	0.814	0.670	0.745	0.792

Compared methods. We compare against three groups of representative baselines. The first group contains unsupervised or training-free quality models, including NIQE [51], VIIDEO [52], STEM [53], and CLIP-IQA [54]. The second group contains supervised VQA/IQA models, including SimpleVQA [55], FAST-VQA [23], DOVER [24], MinimalisticVQA [56], Q-Align [3], and VQA²-Scorer [29]. The third group contains recent reasoning or reinforcement-learning based LMM evaluators, including Q-Insight [5], VisualQuality-R1 [6], VQ-Insight [14], and VQAThinker [7]. For all baselines, we use the official implementations, released checkpoints, or reported settings whenever available, and orient all predicted scores so that larger values indicate better perceptual quality.

Implementation details. VersusQ is initialized from Qwen3-VL-4B-Instruct [38] and augmented with a frozen SlowFast R50 motion encoder [42]. For each video in one pair, we uniformly sample 8 visual frames for the VLM input and extract 64 SlowFast motion tokens. During supervised warm-up, the model is full fine-tuned for one epoch on 18k LSVQ video pairs, with learning rates of 1×10^{-5} for the backbone and 1×10^{-4} for both the motion projector and regression head. In Eq. (10), λ_{reg} is set to 0.5. MC-GRPO, built on GRPO [44], starts from the SFT checkpoint and trains for one epoch on 60k LSVQ pairwise prompts with 4 rollouts per prompt, reward weights 1.0 for margin-regression accuracy and 0.2 for format validity, learning rate 1×10^{-6} , and auxiliary margin weight $\lambda_{\text{aux}} = 0.5$. The visual and motion encoders are frozen. All other trainable modules are optimized with FlashAttention [57] and ZeRO-2 [58].

Table 2: Ablation study of scoring, aggregation, and reasoning optimization on individual VQA benchmarks. The upper and lower panels report SRCC and PLCC, respectively, with higher values indicating better performance.

Variant	In-domain			Out-of-domain					
	LSVQ-Test	LSVQ-1080p	Avg.	KoNViD	LIVE-VQC	YT-Gaming	W-IVC-4K	VDPVE	Avg.
SRCC									
<i>Scoring target</i>									
Pointwise Score (NTP)	0.863	0.786	0.825	0.869	0.780	0.653	0.431	0.683	0.683
Pointwise Score (head)	0.872	0.800	0.836	0.872	0.790	0.704	0.493	0.698	0.711
Pairwise Margin (NTP)	0.877	0.806	0.842	0.871	0.797	0.729	0.516	0.693	0.721
Pairwise Margin (head)	0.884	0.824	0.854	0.879	0.801	0.774	0.587	0.723	0.753
<i>Score recovery from comparisons</i>									
Win-rate Ranking	0.864	0.795	0.829	0.850	0.785	0.737	0.543	0.705	0.724
Elo Rating	0.881	0.814	0.847	0.870	0.799	0.762	0.573	0.717	0.744
Least-squares Recovery	0.884	0.824	0.854	0.879	0.801	0.774	0.587	0.723	0.753
<i>Training recipe (margin target + LSQ)</i>									
SFT w/o Reasoning (18k)	0.851	0.778	0.814	0.815	0.772	0.760	0.331	0.640	0.664
SFT w/ Reasoning (18k)	0.858	0.778	0.818	0.857	0.771	0.710	0.491	0.728	0.711
GRPO from SFT	0.882	0.812	0.847	0.867	0.789	0.779	0.571	0.713	0.744
MC-GRPO from SFT	0.884	0.824	0.854	0.879	0.801	0.774	0.587	0.723	0.753
PLCC									
<i>Scoring target</i>									
Pointwise Score (NTP)	0.863	0.818	0.841	0.880	0.832	0.723	0.423	0.685	0.709
Pointwise Score (head)	0.872	0.832	0.852	0.881	0.840	0.758	0.572	0.704	0.751
Pairwise Margin (NTP)	0.878	0.842	0.860	0.880	0.846	0.777	0.609	0.708	0.764
Pairwise Margin (head)	0.886	0.852	0.869	0.884	0.848	0.814	0.670	0.745	0.792
<i>Score recovery from comparisons</i>									
Win-rate Ranking	0.860	0.820	0.840	0.859	0.821	0.752	0.628	0.726	0.757
Elo Rating	0.880	0.840	0.860	0.877	0.831	0.775	0.657	0.725	0.773
Least-squares Recovery	0.886	0.852	0.869	0.884	0.848	0.814	0.670	0.745	0.792
<i>Training recipe (margin target + LSQ)</i>									
SFT w/o Reasoning (18k)	0.851	0.811	0.831	0.804	0.810	0.782	0.395	0.662	0.691
SFT w/ Reasoning (18k)	0.861	0.819	0.840	0.876	0.828	0.765	0.593	0.740	0.760
GRPO from SFT	0.884	0.840	0.862	0.878	0.836	0.802	0.680	0.732	0.785
MC-GRPO from SFT	0.886	0.852	0.869	0.884	0.848	0.814	0.670	0.745	0.792

4.2 Main Results

Table 1 presents a quantitative comparison of our proposed VersusQ against state-of-the-art baselines, demonstrating its superior alignment with human perception across both in-domain and out-of-domain VQA benchmarks. Overall, VersusQ consistently outperforms existing training-free models, supervised methods, and recent LMM-based methods. Notably, on the in-domain LSVQ dataset, it achieves the highest average performance, showing exceptional robustness on high-definition content (LSVQ-1080p) where it surpasses the strongest LMM baseline by over **3.2%** in rank correlation.

The most significant advantage of VersusQ lies in its remarkable zero-shot generalization capabilities on complex out-of-domain (OOD) datasets. Rather than merely fitting domain-specific data patterns, our method effectively reasons about diverse quality degradations in the wild. For example, on the challenging W-IVC-4K dataset, VersusQ improves PLCC by **7.4%** compared to the latest state-of-the-art VQAThinker. This consistent dominance across varied OOD scenarios validates the superior generalization and reasoning capacity of our proposed approach.

4.3 Ablation Studies

Table 2 studies three design choices: scoring target, score recovery, and training recipe, with all variants evaluated on both in-domain and out-of-domain benchmarks.

Scoring target. Pairwise margin prediction consistently outperforms pointwise score prediction, indicating that relative comparisons provide more transferable supervision than dataset-calibrated absolute scores. Using a regression head further improves over NTP decoding by directly modeling continuous quality gaps, which motivates our final pairwise-margin formulation.

Score recovery from margins. Compared with win-rate ranking [8] and Elo rating [59], least-squares recovery better exploits the predicted margins by preserving their signed magnitudes and solving all pairwise constraints jointly. We therefore use anchor-free least-squares aggregation as the default recovery rule for VersusQ.

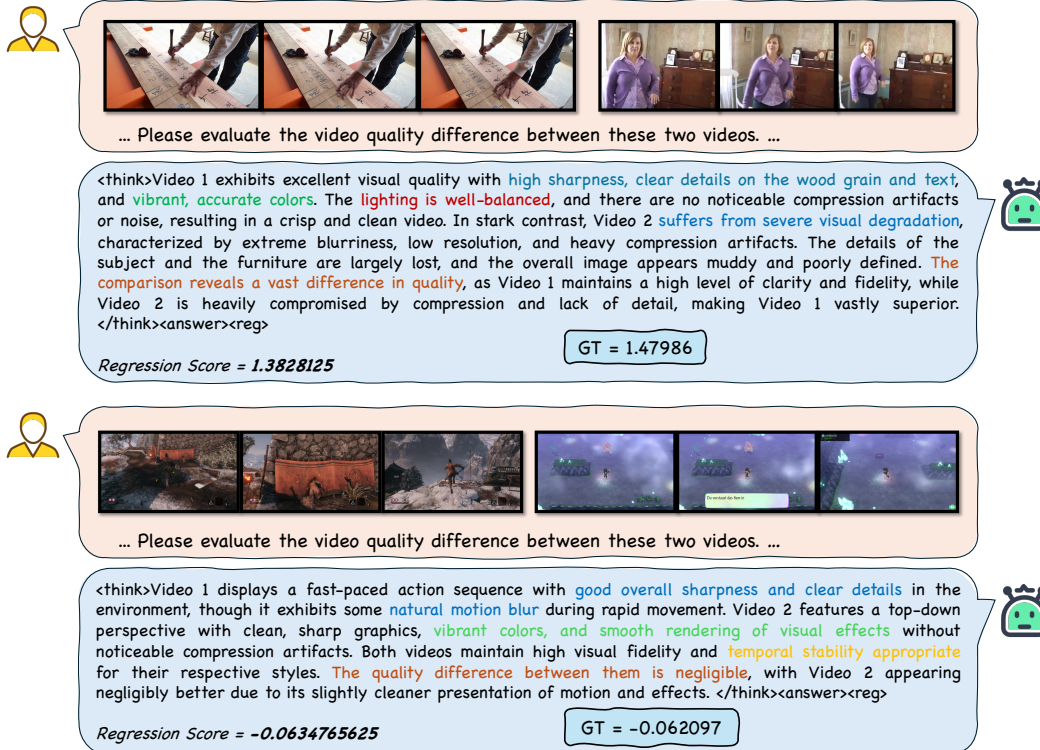


Figure 3: **Qualitative case study of VersusQ on video pairs.** The model first produces comparison-oriented reasoning and then predicts a continuous regression margin aligned with the ground-truth quality difference.

Training recipe. The lower panel studies how reasoning supervision and reinforcement optimization affect the margin-based model. Reasoning supervision improves transfer by encouraging the model to ground margin prediction in explicit perceptual evidence rather than shortcut score fitting. GRPO further strengthens ranking consistency through rollout-based optimization, while MC-GRPO provides the most reliable recipe by keeping the reasoning policy aligned with the continuous regression head. Overall, the ablation confirms that comparison rationales, reinforcement learning, and margin-coupled updates are complementary components of the final training pipeline.

4.4 Qualitative Analysis

Figure 3 presents a representative comparison case from the evaluation set. The generated rationale contrasts concrete visual evidence from the two videos, including sharpness, color fidelity, lighting, and compression artifacts, while the regression head produces a continuous margin close to the ground-truth score difference.

5 Conclusion

This paper presented VersusQ, a pairwise margin reasoning framework for generalizable video quality assessment with large multimodal models. VersusQ shifts VQA from pointwise absolute score fitting to direct video comparison, where the model reasons about visual and temporal quality differences and predicts a signed continuous margin. These local margins are then consolidated into globally comparable quality scores through anchor-free least-squares recovery. To bridge interpretable relational rationales and fine-grained numerical differences, VersusQ further introduces MC-GRPO, which jointly optimizes rollout-based reasoning and continuous margin regression. Experiments across seven public VQA benchmarks show that this design achieves state-of-the-art performance, improves cross-domain generalization, and provides reliable fine-grained ranking under heterogeneous evaluation scenarios. Future work will explore more efficient pair selection and stronger temporal modeling for long-form or AIGC video quality assessment.

References

- [1] Xionghuo Min, Huiyu Duan, Wei Sun, Yucheng Zhu, and Guangtao Zhai. Perceptual video quality assessment: A survey. *Science China Information Sciences*, 67(11):211301, 2024.
- [2] Guangtao Zhai and Xionghuo Min. Blind image quality assessment: A survey on blind image quality assessment. *IEEE Transactions on Pattern Analysis and Machine Intelligence*, 45(5): 5833–5857, 2023.
- [3] Haoning Wu, Zicheng Zhang, Weixia Zhang, Chaofeng Chen, Liang Liao, Chunyi Li, Yixuan Gao, Annan Wang, Erli Zhang, Wenxiu Sun, Qiong Yan, Xionghuo Min, Guangtao Zhai, and Weisi Lin. Q-align: Teaching llms for visual scoring via discrete text-defined levels. In *Proceedings of the 41st International Conference on Machine Learning (ICML)*, 2024.
- [4] Zhiyuan You, Xin Cai, Jinjin Gu, Tianfan Xue, and Chao Dong. Teaching large language models to regress accurate image quality scores using score distribution. In *Proceedings of the IEEE/CVF Conference on Computer Vision and Pattern Recognition (CVPR)*, 2025.
- [5] Weiqi Li, Xuanyu Zhang, Shijie Zhao, Yabin Zhang, Junlin Li, Li Zhang, and Jian Zhang. Q-insight: Understanding image quality via visual reinforcement learning. In *Advances in Neural Information Processing Systems (NeurIPS)*, 2025.
- [6] Tianhe Wu, Jian Zou, Jie Liang, Lei Zhang, and Kede Ma. Visualquality-r1: Reasoning-induced image quality assessment via reinforcement learning to rank. In *Advances in Neural Information Processing Systems (NeurIPS)*, 2025.
- [7] Chunyi Cao, Wei Sun, Zicheng Zhang, Yingjie Jia, Xiaohong Liu, Xionghuo Min, and Guangtao Zhai. Vqathinker: Exploring generalizable and explainable video quality assessment via reinforcement learning. In *Proceedings of the AAAI Conference on Artificial Intelligence (AAAI)*, 2026.
- [8] Ralph Allan Bradley and Milton E Terry. Rank analysis of incomplete block designs: I. the method of paired comparisons. *Biometrika*, 39(3/4):324–345, 1952.
- [9] Chris Burges, Tal Shaked, Erin Renshaw, Ari Lazier, Matt Deeds, Nicole Hamilton, and Greg Svore. Learning to rank using gradient descent. In *Proceedings of the 22nd International Conference on Machine Learning (ICML)*, pages 89–96, 2005.
- [10] Tie-Yan Liu. Learning to rank for information retrieval. *Foundations and Trends in Information Retrieval*, 3(3):225–331, 2009.
- [11] Xialei Liu, Joost van de Weijer, and Andrew D Bagdanov. Rankiq: Learning from rankings for no-reference image quality assessment. In *Proceedings of the IEEE International Conference on Computer Vision (ICCV)*, pages 1040–1049, 2017.
- [12] Hanwei Zhu, Haoning Wu, Yixuan Li, Zicheng Zhang, Baoliang Chen, Lingyu Zhu, Yuming Fang, Guangtao Zhai, Weisi Lin, and Shiqi Wang. Adaptive image quality assessment via teaching large multimodal models to compare. In *Advances in Neural Information Processing Systems (NeurIPS)*, 2024.
- [13] Jiarui Zhang, Mahyar Khayatkhoei, Prateek Chhikara, and Filip Ilievski. Mllms know where to look: Training-free perception of small visual details with multimodal llms. In *International Conference on Learning Representations (ICLR)*, 2025.
- [14] Xuanyu Zhang, Weiqi Li, Shijie Zhao, Junlin Li, Li Zhang, and Jian Zhang. Vq-insight: Teaching vlms for ai-generated video quality understanding via progressive visual reinforcement learning. In *Proceedings of the AAAI Conference on Artificial Intelligence (AAAI)*, 2026.
- [15] Xiaoye Jiang, Lek-Heng Lim, Yuan Yao, and Yinyu Ye. Statistical ranking and combinatorial Hodge theory. *Mathematical Programming*, 127(1):203–244, 2011. doi: 10.1007/s10107-010-0419-x.
- [16] Zhou Wang, Alan C Bovik, Hamid R Sheikh, and Eero P Simoncelli. Image quality assessment: from error visibility to structural similarity. *IEEE transactions on image processing*, 13(4): 600–612, 2004.

- [17] Kalpana Seshadrinathan, Rajiv Soundararajan, Alan C Bovik, and Lawrence K Cormack. Motion-based perceptual quality assessment of video. *IEEE Transactions on Image Processing*, 19(2):335–350, 2010.
- [18] Zhi Li, Anne Aaron, Ioannis Katsavounidis, Anush Moorthy, and Megha Manohara. Toward a practical perceptual video quality metric. In *The Netflix Tech Blog*, 2016.
- [19] Rajiv Soundararajan and Alan C Bovik. Video quality assessment by reduced reference spatio-temporal entropic differencing. *IEEE Transactions on Circuits and Systems for Video Technology*, 23(4):684–694, 2013.
- [20] Le Kang, Peng Ye, Yi Li, and David Doermann. Convolutional neural networks for no-reference image quality assessment. In *Proceedings of the IEEE Conference on Computer Vision and Pattern Recognition (CVPR)*, pages 1733–1740, 2014.
- [21] Weixia Zhang, Kede Ma, Jia Yan, Dexiang Deng, and Zhou Wang. Blind image quality assessment using a deep bilinear convolutional neural network. *IEEE Transactions on Circuits and Systems for Video Technology*, 30(1):36–47, 2020.
- [22] Dingquan Li, Tingting Jiang, and Ming Jiang. Quality assessment of in-the-wild videos. In *Proceedings of the 27th ACM International Conference on Multimedia (ACM MM)*, pages 2351–2359, 2019.
- [23] Haoning Wu, Chaofeng Chen, Jingwen Hou, Liang Liao, Annan Wang, Wenxiu Sun, Qiong Yan, and Weisi Lin. Fast-vqa: Efficient end-to-end video quality assessment with fragment sampling. In *Proceedings of the European Conference on Computer Vision (ECCV)*, 2022.
- [24] Haoning Wu, Erli Zhang, Liang Liao, Chaofeng Chen, Jingwen Hou, Annan Wang, Wenxiu Sun, Qiong Yan, and Weisi Lin. Exploring video quality assessment on user generated contents from aesthetic and technical perspectives. In *Proceedings of the IEEE/CVF International Conference on Computer Vision (ICCV)*, 2023.
- [25] Yunpeng Qu, Kun Yuan, Qizhi Xie, Ming Sun, Chao Zhou, and Jian Wang. KVQ: Boosting video quality assessment via saliency-guided local perception. In *Proceedings of the IEEE/CVF Conference on Computer Vision and Pattern Recognition (CVPR)*, 2025.
- [26] Haotian Liu, Chunyuan Li, Qingyang Wu, and Yong Jae Lee. Visual instruction tuning. In *Advances in Neural Information Processing Systems (NeurIPS)*, 2023.
- [27] Zhe Chen, Jiannan Wu, Wenhai Wang, Weijie Su, Guo Chen, Sen Xing, Muyan Zhong, Qionglong Zhang, Xizhou Zhu, Lewei Lu, et al. Internvl: Scaling up vision foundation models and aligning for generic visual-linguistic tasks. In *Proceedings of the IEEE/CVF Conference on Computer Vision and Pattern Recognition (CVPR)*, 2024.
- [28] Jinze Bai, Shuai Bai, Shusheng Yang, Shijie Wang, Sinan Tan, Peng Wang, Junyang Lin, Chang Zhou, and Jingren Zhou. Qwen-vl: A versatile vision-language model for understanding, localization, text reading, and beyond. *arXiv preprint arXiv:2308.12966*, 2023.
- [29] Ziheng Jia, Zicheng Zhang, Jiaying Qian, Haoning Wu, Wei Sun, Chunyi Li, Xiaohong Liu, Weisi Lin, Guangtao Zhai, and Xiongkuo Min. Vqa²: Visual question answering for video quality assessment. In *Proceedings of the 33rd ACM International Conference on Multimedia (ACM MM)*, 2025.
- [30] Shijie Zhao, Xuanyu Zhang, Weiqi Li, Junlin Li, Li Zhang, Tianfan Xue, and Jian Zhang. Reasoning as representation: Rethinking visual reinforcement learning in image quality assessment. In *Proceedings of the International Conference on Learning Representations (ICLR)*, 2026.
- [31] Paul F Christiano, Jan Leike, Tom Brown, Miljan Martic, Shane Legg, and Dario Amodei. Deep reinforcement learning from human preferences. In *Advances in Neural Information Processing Systems (NeurIPS)*, volume 30, 2017.
- [32] Long Ouyang, Jeffrey Wu, Xu Jiang, Diogo Almeida, Carroll Wainwright, Pamela Mishkin, Chong Zhang, Sandhini Agarwal, Katarina Slama, Alex Ray, et al. Training language models to follow instructions with human feedback. *Advances in Neural Information Processing Systems (NeurIPS)*, 35:27730–27744, 2022.

- [33] Zhihong Shao, Peiyi Wang, Qihao Zhu, Runxin Xu, Junxiao Song, Xiao Bi, Haowei Zhang, Mingchuan Zhang, Y. K. Li, Y. Wu, et al. Deepseekmath: Pushing the limits of mathematical reasoning in open language models. *arXiv preprint arXiv:2402.03300*, 2024.
- [34] DeepSeek-AI. Deepseek-r1: Incentivizing reasoning capability in llms via reinforcement learning. *arXiv preprint arXiv:2501.12948*, 2025.
- [35] Kaituo Feng, Kaixiong Gong, Bohao Li, Zonghao Guo, Yibing Wang, Tianshuo Peng, Junfei Wu, Xiaoying Zhang, Benyou Wang, and Xiangyu Yue. Video-r1: Reinforcing video reasoning in mllms. In *Advances in Neural Information Processing Systems (NeurIPS)*, 2025.
- [36] Kaituo Feng, Manyuan Zhang, Hongyu Li, Kaixuan Fan, Shuang Chen, Yilei Jiang, Dian Zheng, Peiwen Sun, Yiyuan Zhang, Haoze Sun, Yan Feng, Peng Pei, Xunliang Cai, and Xiangyu Yue. Onethinker: All-in-one reasoning model for image and video. *arXiv preprint arXiv:2512.03043*, 2025.
- [37] Weiyun Wang, Zhangwei Gao, Lixin Gu, Hengjun Pu, Long Cui, Xingguang Wei, Zhaoyang Liu, Linglin Jing, Shenglong Ye, Jie Shao, et al. Internvl3.5: Advancing open-source multimodal models in versatility, reasoning, and efficiency. *arXiv preprint arXiv:2508.18265*, 2025.
- [38] Shuai Bai, Yuxuan Cai, Ruizhe Chen, Keqin Chen, Xionghui Chen, Zesen Cheng, Lianghao Deng, Wei Ding, Chang Gao, Chunjiang Ge, et al. Qwen3-vl technical report. *arXiv preprint arXiv:2511.21631*, 2025.
- [39] Ziyu Liu, Zhiqian Sun, Yifan Li, Zhi Wang, Haotian Guo, Peng Yuan, Nan Shen, Fan Yang, and Zheng Yu. Visual-rft: Visual reinforcement fine-tuning. In *Proceedings of the IEEE/CVF International Conference on Computer Vision (ICCV)*, 2025.
- [40] Jiahui Yang, Hao Dong, Sen Wang, Yi Wang, and Guansong Xia. R1-onevision: Advancing generalized multimodal reasoning through cross-modal formalization. *arXiv preprint arXiv:2503.12478*, 2025.
- [41] Peng Liu, Kai Luo, Jiayuan Zheng, Enze Xie, and Zhenguo Li. Seg-zero: Reasoning-chain guided segmentation via cognitive reinforcement. *arXiv preprint arXiv:2503.06520*, 2025.
- [42] Christoph Feichtenhofer, Haoqi Fan, Jitendra Malik, and Kaiming He. Slowfast networks for video recognition. In *Proceedings of the IEEE/CVF International Conference on Computer Vision (ICCV)*, pages 6202–6211, 2019.
- [43] Google DeepMind. Gemini 3 pro model evaluation, 2025. https://storage.googleapis.com/deepmind-media/gemini/gemini_3_pro_model_evaluation.pdf.
- [44] Zhihong Shao, Peiyi Wang, Qihao Zhu, Runxin Xu, Junxiao Song, Xiao Bi, Haowei Zhang, Mingchuan Zhang, Y. K. Li, Y. Wu, et al. Deepseekmath: Pushing the limits of mathematical reasoning in open language models. *arXiv preprint arXiv:2402.03300*, 2024.
- [45] Zhenqiang Ying, Maitreya Manivasagam, Hasnain Mannan, Eero P Simoncelli, and Alan C Bovik. Patch-vq: ‘patching up’ the video quality problem. In *Proceedings of the IEEE/CVF Conference on Computer Vision and Pattern Recognition (CVPR)*, pages 14019–14029, 2021.
- [46] Vlad Hosu, Franz Hahn, Mohsen Jenadeleh, Hanhe Lin, Hui Men, Tamás Szirányi, Shujun Li, and Dietmar Saupe. The konstanz natural video database (konvid-1k). In *2017 Ninth International Conference on Quality of Multimedia Experience (QoMEX)*, pages 1–6. IEEE, 2017.
- [47] Zeina Sinno and Alan C. Bovik. Large-scale study of perceptual video quality. *IEEE Transactions on Image Processing*, 28(2):612–627, 2019. doi: 10.1109/TIP.2018.2869673.
- [48] Xiangxu Yu, Zhengzhong Tu, Neil Birkbeck, Yilin Wang, Balu Adsumilli, and Alan C. Bovik. Perceptual quality assessment of ugc gaming videos. *arXiv preprint arXiv:2204.00128*, 2022.
- [49] Zhuoran Li, Zhengfang Duanmu, Wentao Liu, and Zhou Wang. Avc, hev1, vp9, avs2 or av1? a comparative study of state-of-the-art video encoders on 4k videos. In *16th International Conference on Image Analysis and Recognition (ICIAR)*, 2019.

- [50] Yixuan Gao, Yuqin Cao, Tengchuan Kou, Wei Sun, Yunlong Dong, Xiaohong Liu, Xiongkuo Min, and Guangtao Zhai. Vdpve: Vqa dataset for perceptual video enhancement. In *Proceedings of the IEEE/CVF Conference on Computer Vision and Pattern Recognition Workshops (CVPRW)*, pages 1474–1483, 2023.
- [51] Anish Mittal, Rajiv Soundararajan, and Alan C Bovik. Making a “completely blind” image quality analyzer. *IEEE Signal Processing Letters*, 20(3):209–212, 2013.
- [52] Anish Mittal, Michele A. Saad, and Alan C. Bovik. A completely blind video integrity oracle. *IEEE Transactions on Image Processing*, 25(1):289–300, 2016. doi: 10.1109/TIP.2015.2502725.
- [53] Parimala Kancharla and Sumohana S. Channappayya. Completely blind quality assessment of user generated video content. *IEEE Transactions on Image Processing*, 31:263–274, 2022. doi: 10.1109/TIP.2021.3130541.
- [54] Jianyi Wang, Kelvin C. K. Chan, and Chen Change Loy. Exploring clip for assessing the look and feel of images. In *Proceedings of the AAAI Conference on Artificial Intelligence (AAAI)*, 2023.
- [55] Wei Sun, Xiongkuo Min, Wei Lu, and Guangtao Zhai. A deep learning based no-reference quality assessment model for ugc videos. In *Proceedings of the 30th ACM International Conference on Multimedia (ACM MM)*, pages 856–865, 2022.
- [56] Wei Sun, Wen Wen, Xiongkuo Min, Long Lan, Guangtao Zhai, and Kede Ma. Analysis of video quality datasets via design of minimalistic video quality models. *IEEE Transactions on Pattern Analysis and Machine Intelligence*, 2024.
- [57] Tri Dao, Daniel Y. Fu, Stefano Ermon, Atri Rudra, and Christopher Ré. Flashattention: Fast and memory-efficient exact attention with io-awareness. In *Advances in Neural Information Processing Systems (NeurIPS)*, 2022.
- [58] Samyam Rajbhandari, Jeff Rasley, Olatunji Ruwase, and Yuxiong He. Zero: Memory optimizations toward training trillion parameter models. In *SC20: International Conference for High Performance Computing, Networking, Storage and Analysis*, 2020.
- [59] Arpad E. Elo. *The Rating of Chessplayers, Past and Present*. Arco Publishing, 1978.

A Sparse Graph Analysis

Sparse graph construction. For a benchmark with N videos, the evaluation graph is an undirected sparse comparison graph $\mathcal{G} = (\mathcal{V}, \mathcal{E})$, where each vertex is a test video and each queried unordered pair becomes one edge. The edge orientation is assigned only when forming the linear system, so an edge $e = (i, j)$ contributes $s_i - s_j \approx \hat{m}_{ij}$. Pair selection proceeds in batches. The sampler prioritizes low-degree vertices, then selects a partner either from the same score quantile or from a local rating window so that compared videos are neither trivially different nor disconnected from the rest of the graph. Duplicate unordered pairs within a batch are removed. After each batch, match counts and provisional ratings are updated, and the next batch is sampled from the updated graph state. This yields $M = |\mathcal{E}|$ comparisons with $M \ll N(N - 1)/2$, while preserving enough connectivity for the zero-mean least-squares recovery in Eq. (5).

Sparse Graph Convergence Analysis Figure 4 analyzes how many sparse-graph edges are required before the recovered leaderboard becomes stable.

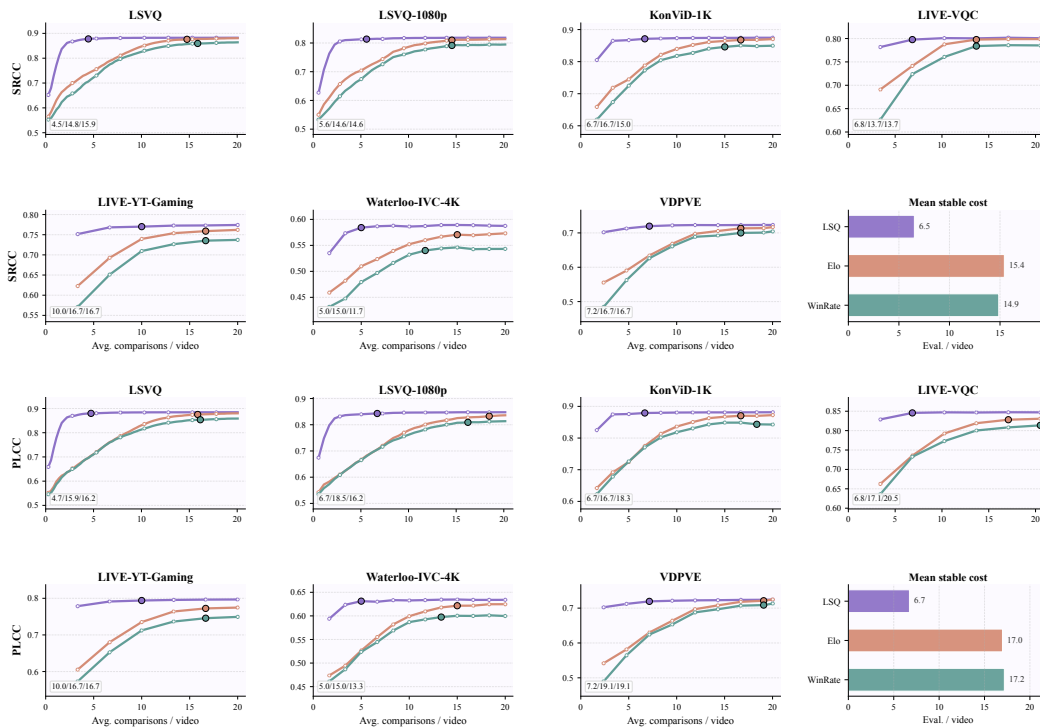


Figure 4: **Convergence of sparse-graph leaderboard reconstruction.** Curves are computed from prefixes of the sampled comparison-edge stream on the seven reported benchmarks. A method is marked stable for each metric once the corresponding SRCC or PLCC is within 0.005 of its final value, where SRCC denotes Spearman rank correlation coefficient and PLCC denotes Pearson linear correlation coefficient. LSQ denotes least-squares aggregation. LSQ reaches stable correlation with fewer comparisons on most datasets because it uses the signed margin magnitude on every sparse-graph edge, whereas Elo and win-rate aggregation rely mainly on preference outcomes.

The convergence curves indicate that a sparse comparison graph is sufficient for stable leaderboard reconstruction. Across the seven benchmarks, LSQ reaches the 0.005 stability band with substantially fewer pairwise evaluations than Elo and win-rate aggregation in most cases. The reason is that LSQ uses the signed margin magnitude on every queried edge, while outcome-only methods reduce each comparison to a binary or ternary preference. As a result, each LSQ edge provides both the preference direction and the calibrated quality gap, giving the least-squares system stronger constraints for recovering global scores. These results support the sparse-graph design in Sec. A. Once the graph covers most videos and maintains moderate local connectivity, the system can average noisy pairwise

margins and recover a stable ordering without evaluating the dense all-pairs graph. Based on this convergence behavior, we use a fixed sparse-evaluation budget of $5N$ pairwise comparisons for a benchmark with N videos when reporting the final results. Because each comparison contains two videos, this budget gives each video an average degree of about ten in the comparison graph, providing a consistent trade-off between reconstruction stability and evaluation cost across benchmarks.

B Additional Experimental Details

Training details. Unless otherwise noted, all experiments were conducted using NVIDIA A800 GPUs (80GB). During the supervised warm-up stage, the model was trained for two epochs on a single 8-GPU node with a global batch size of 8 video pairs, using the signed-margin tensor as a direct input to compute the hybrid CoT-regression loss. The subsequent MC-GRPO stage utilized a four-node setup: one 8-GPU node dedicated to asynchronous vLLM rollouts and three for distributed optimization. This stage involved training on 60k prompts for a single epoch, with a global batch size of 48 and a KL coefficient of 0.01.

Ablation setup. (1) Regarding the scoring target analysis, both the pointwise and pairwise methods utilize a data size ratio of approximately 1:4 between the supervised warm-up and GRPO stages. (2) In the analysis of score recovery from comparisons, we define a margin threshold of 0.2, treating any score difference less than 0.2 as a draw when aggregating pairwise comparisons into rankings via win rates and Elo. This introduces a valuable fault-tolerance mechanism, proving more effective than a rigid zero-tolerance setting. (3) Focusing on the training recipes, the two SFT models (with and without reasoning) utilize identical data and training configurations, differing solely in the inclusion of CoT rationales. During GRPO training based on the SFT model, the regression head for scoring margin is kept frozen.

C CoT Annotation Prompt

We use Gemini-3-Pro [43] to generate chain-of-thought style rationales for pairwise video quality comparisons. This process produces an 18k-pair CoT annotation set, which will be made publicly available upon acceptance. To make the annotation procedure reproducible, we summarize the construction of the prompt fields in the pseudocode below and then present the full prompt template.

Descriptor Rules for Pairwise Quality Margins

```
diff = video1_score - video2_score

# direction_desc: which video is better
if diff > 0: direction_desc = "Video 1 is better"
elif diff < 0: direction_desc = "Video 2 is better"
else:
    direction_desc = "the two videos are equal in quality"

# score_diff_str: signed numeric value of diff with two decimals
score_diff_str = format(diff, "+.2f")

# (magnitude_desc, degree_word, forbidden_words) by bin of |diff|
if |diff| < 0.1:
    magnitude_desc = "very similar"
    degree_word = "negligible"
    forbidden_words = "Avoid: slight, moderate, noticeable, significant, vast."
elif 0.1 <= |diff| < 0.3:
    magnitude_desc = "slightly different"
    degree_word = "slightly"
    forbidden_words = "Avoid: negligible, moderate, noticeable, significant, vast."
elif 0.3 <= |diff| < 0.6:
    magnitude_desc = "moderately different"
    degree_word = "moderately"
    forbidden_words = "Avoid: slight, marginal, a bit, negligible, vast."
```

```

elif 0.6 <= |diff| < 1.0:
    magnitude_desc = "significantly different"
    degree_word    = "significantly"
    forbidden_words = "Avoid: slight, moderate, negligible, marginal."
elif |diff| >= 1.0
    magnitude_desc = "very different"
    degree_word    = "vastly"
    forbidden_words = "Avoid: slight, moderate, somewhat, marginal."

```

Pairwise CoT Annotation Prompt

You are an expert video quality assessor. You are given two videos (each represented as a 3x3 grid of sampled frames showing temporal progression) and asked to evaluate their overall visual quality difference.

Image 1: Video 1's 3x3 frame grid (9 frames sampled uniformly across time)

Image 2: Video 2's 3x3 frame grid (9 frames sampled uniformly across time)

The scoring system: Each video has a quality score ranging from 1 to 5. The score difference is computed as (Video 1 score minus Video 2 score), ranging from -4 to 4.

- Positive value → Video 1 is better
- Negative value → Video 2 is better
- Value close to 0 → similar quality

The ground truth score difference is `**{score_diff_str}**`, meaning the two videos are `{magnitude_desc}` and `{direction_desc}`.

The magnitude scale for reference (score difference on a 1-5 scale):

- $|diff| < 0.1$ → negligible difference (nearly identical)
- $0.1 \leq |diff| < 0.3$ → slight difference (small gap)
- $0.3 \leq |diff| < 0.6$ → moderate difference (clear, meaningful gap)
- $0.6 \leq |diff| < 1.0$ → significant difference (large, obvious gap)
- $|diff| \geq 1.0$ → vast difference (huge quality gap)

Please analyze both videos and generate a detailed reasoning that justifies the score difference of `{score_diff_str}`.

Your response MUST be in valid JSON format, following this EXACT structure (no extra text or markdown formatting outside the JSON block):

```

{
  "score_difference": "{score_diff_str}",
  "reasoning": "[Your detailed analysis here. Include: 1. Description of Video 1's key visual quality characteristics (e.g., sharpness, noise, compression artifacts, color accuracy, temporal stability, exposure, motion blur) 2. Description of Video 2's key visual quality characteristics 3. Comparative analysis explaining why the two videos are {magnitude_desc} and {direction_desc}]"
}

```

Important rules:

- The reasoning must be genuine and based on what you observe in the frame grids
- Keep the reasoning concise but informative
- Focus on overall video quality aspects: sharpness, noise/grain, compression artifacts, color fidelity, exposure, temporal consistency, motion blur, etc.
- The degree/magnitude words in your reasoning MUST match the actual score difference. Use `{degree_word}` to describe the difference. `{forbidden_words}`
- Ignore any subtitles, captions, watermarks, or overlaid text present in the video frames, focus only on the visual content itself
- Write in English

D Limitations and Discussions

VersusQ reduces dense all-pairs evaluation through sparse pairwise comparisons, but leaderboard construction still requires multiple model calls per test video. The recovered scores also inherit the coverage and reliability of the sparse comparison graph. In addition, training and evaluation use MOS-based public VQA benchmarks, so residual dataset bias, annotation noise, and annotator disagreement may still affect the learned quality scale. Since pairwise preferences are generally more reliable and consistent than absolute MOS ratings, a promising direction for future work is to build dedicated pairwise comparison training sets to mitigate these biases.

E Additional Qualitative Analysis

Figures 5 and 6 provide examples of the comparison-style output. The rationale first separates perceptual evidence for the two videos and then summarizes the quality gap before the regression head predicts the signed margin. This format makes the ranking decision auditable while preserving a continuous output for leaderboard reconstruction.



Figure 5: **Additional qualitative case study.** The case illustrates comparison-oriented reasoning for a video pair, followed by a continuous regression margin aligned with the ground-truth quality difference.



Figure 6: **Additional qualitative case study.** The case provides another example of comparison-oriented reasoning for a video pair, followed by a continuous regression margin aligned with the ground-truth quality difference.